

Seismic lateral earth pressure analysis of retaining walls

Muhammad Ismeik^{*1,2} and Fathi Shaqour³

¹ Department of Civil Engineering, The University of Jordan, Amman 11942, Jordan

² Department of Civil Engineering, Australian College of Kuwait, Safat 13015, Kuwait

³ Department of Applied Geology and Environment, The University of Jordan, Amman 11942, Jordan

(Received September 30, 2013, Revised April 22, 2014, Accepted December 13, 2014)

Abstract. Based on limit equilibrium principles, this study presents a theoretical derivation of a new analytical formulation for estimating magnitude and lateral earth pressure distribution on a retaining wall subjected to seismic loads. The proposed solution accounts for failure wedge inclination, unit weight and friction angle of backfill soil, wall roughness, and horizontal and vertical seismic ground accelerations. The current analysis predicts a nonlinear lateral earth pressure variation along the wall with and without seismic loads. A parametric study is conducted to examine the influence of various parameters on lateral earth pressure distribution. Findings reveal that lateral earth pressure increases with the increase of horizontal ground acceleration while it decreases with the increase of vertical ground acceleration. Compared to classical theory, the position of resultant lateral earth force is located at a higher distance from wall base which in turn has a direct impact on wall stability and economy. A numerical example is presented to illustrate the computations of lateral earth pressure distribution based on the suggested analytical method.

Keywords: lateral earth pressure; limit equilibrium; seismic stability; retaining wall; theoretical analysis

1. Introduction

Retaining walls are common structures of civil engineering. The major function of such structures is to retain unsupported soil for vertical cuts of excavations. Typical applications include road cuts, water structures, landscaping, port and building construction.

Theoretical analysis is generally used in geotechnical engineering for predicting soil behavior under various conditions. Typical successful applications include soil reinforcement (Perkins *et al.* 1998), soil modeling (Ismeik and Al-Rawi 2014), consolidation analysis (Ismeik 2012a, b), soil stabilization (Ismeik *et al.* 2013), and determination of lateral pressure against retaining walls using limit equilibrium methods (Sokolowskii 1965, Lee and Herrington 1972).

A comprehensive design of a retaining wall requires an estimate of pressure distribution along the wall which in turn affects its stability, safety, and economy. The most classical theories used to determine such a pressure were initially proposed by Coulomb (1776) and Rankine (1857). Other approaches based on limit equilibrium, charts, analytical formulations, graphical construction techniques, and some numerical methods were traditionally used to estimate lateral earth pressure under static loads (Terzaghi 1943, Caquot and Kerisel 1948, Sherif *et al.* 1982, Bang 1985, Chen and Liu 1990, Bowels 1996).

*Corresponding author, Ph.D., E-mail: ismeik@ju.edu.jo; m.ismeik@ack.edu.kw

In addition to gravitational loads, the proper determination of seismic lateral earth pressure and its distribution is required when a retaining wall is located at an earthquake-prone zone. This is a crucial issue for its safe design since earthquake induced loads may cause large damages to retaining structures with physical and economic consequences.

Seismic lateral earth pressure estimation against a retaining wall has been investigated by many researchers. Based on the pseudo static approach, pioneering works by Okabe (1926) and Mononobe and Matsuo (1929), known commonly as Mononobe-Okabe (M-O) method, is traditionally used by geotechnical engineers to compute lateral earth pressure distribution against retaining walls. The method is a straightforward extension of the Coulomb (1776) theory to pseudo static conditions in which seismic loads are accounted for by applying horizontal and vertical inertia forces to an assumed failure wedge. In addition to M-O method, researchers have developed other methods to determine the seismic lateral earth pressure acting on a retaining wall based on different theories and assumptions. Major studies include Das and Puri (1996), Dewaikar and Halkude (2002), Choudhury and Singh (2005), Choudhury and Nimbalkar (2006), Shukla *et al.* (2009), Basha and Babu (2010), Ghosh and Sharma (2010), and Shukla and Zahid (2011).

Among different approaches, the horizontal slice method (HSM) has been used to compute the lateral earth pressure against a retaining wall. The method was initially developed by Shahgholi *et al.* (2001) and used by Nouri *et al.* (2006), Nouri *et al.* (2008), Shekarian *et al.* (2008), Ahmadabadi and Ghanbari (2009), and Ghanbari and Taheri (2012) to determine lateral earth pressure distribution mostly in reinforced soil applications. In addition, Wang (2000), and Wang *et al.* (2004) used this method to determine earth pressure distribution on a retaining wall where only static forces were considered.

Based on the above literature review and up to authors' knowledge, an approach for lateral earth pressure estimation against retaining walls, subjected to seismic loads in the framework of pseudo static analysis and using HSM, is not yet available. In this research, an effort is made to develop a new analytical expression for predicting lateral earth pressure distribution behind a retaining wall with relation to horizontal and vertical earthquake accelerations. The complete theoretical derivation of the proposed method is presented based on limit equilibrium principals for a vertical retaining wall, tilting about its top, and supporting a granular soil. A parametric study is conducted to investigate the effect of soil and wall properties variation, and seismic loading conditions, on lateral earth pressure distribution along the retaining wall depth.

2. Mathematical formulation

A vertical retaining wall with height H is shown in Fig. 1. The failure surface is considered to be a plane and passing through wall heel with a width B and an inclination angle ρ ($\cot^{-1} B/H$) to the horizontal. The backfill consists of a leveled homogeneous, elastic, and isotropic granular soil with a friction angle ϕ , unit weight γ , and wall-to-soil friction angle δ . An arbitrary horizontal infinitesimal soil element, located at a depth z with the orientation of forces acting on it, is considered per unit length of wall. The applied forces acting on this differential soil include internal vertical force V , shearing force at the top of soil element F , shearing forces S_1 and S_2 , and normal compressive forces C_1 and C_2 , acting on the two sides of element, weight of soil W , and horizontal and vertical seismic inertia force components Q_h and Q_v , respectively. To simplify the derivation, the proposed method is based on limit equilibrium concept where parabolic or higher order terms are ignored.

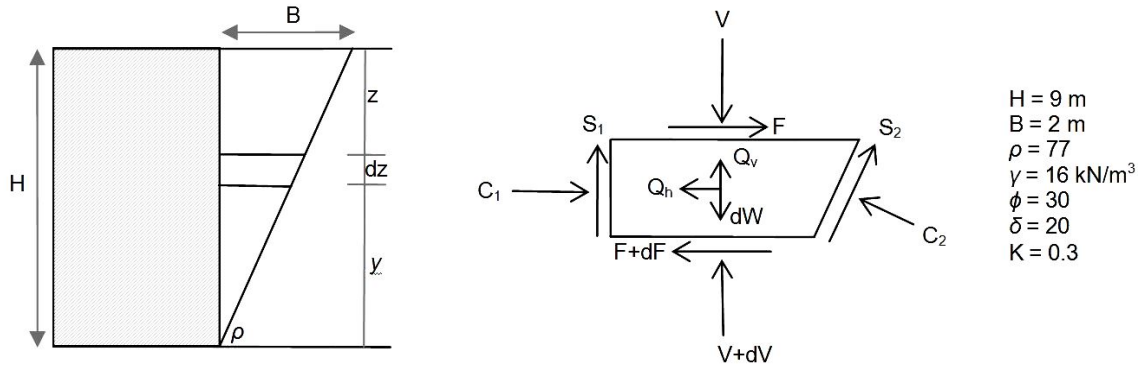


Fig. 1 Wall model, differential soil element free body diagram, and parametric study input data

As suggested by M-O theory, the inertia forces Q_h and Q_v are defined as

$$Q_h = k_h dW \tag{1}$$

$$Q_v = k_v dW \tag{2}$$

where k_h and k_v are horizontal and vertical seismic ground acceleration coefficients, respectively, and dW is the differential weight of soil element. Positive sign is used for vertically upwards direction of k_v and for horizontally towards wall direction of k_h as illustrated in Fig. 1. The relationships between shearing and normal forces acting on soil element are assumed to be

$$S_1 = C_1 \tan \delta \tag{3}$$

$$S_2 = C_2 \tan \phi \tag{4}$$

$$F = V \tan \phi \tag{5}$$

The horizontal pressure at any particular depth z is determined as

$$\sigma_H = K \sigma_V \tag{6}$$

where σ_H and σ_V are horizontal and vertical pressures, and K is lateral earth pressure coefficient. Since the infinitesimal area dA can be determined from soil element geometry, the soil differential weight dW is then calculated as

$$dW = \gamma dA = \gamma \cot \rho (H - z) dz \tag{7}$$

With vertical pressure definition σ_V given by Eq. (8), the differential vertical force dV is calculated as shown in Eq. (9). Namely

$$\sigma_V = \frac{V}{(H - z + dz) \cot \rho} \tag{8}$$

$$dV = \cot \rho [(H - z) d\sigma_V - \sigma_V dz] \tag{9}$$

Table 1 List of unknowns and equations used within the proposed method

Unknowns	Equations
C_1	$S_1 = C_1 \tan \delta$
C_2	$S_2 = C_2 \tan \phi$
S_1	$F = V \tan \phi$
S_2	$\sigma_H = K \sigma_V$
V	$\Sigma F_H = 0$
F	$\Sigma F_V = 0$
6	6

Using Eqs. (6) and (10) as the definition of the horizontal pressure σ_H , wall-to-soil normal compressive force C_1 is calculated by Eq. (11). That is

$$\sigma_H = \frac{C_1}{dz} \quad (10)$$

$$C_1 = \sigma_H dz = K \sigma_V dz \quad (11)$$

Writing the horizontal equilibrium equation of forces yields

$$F + C_1 + S_2 \cos \rho = C_2 \sin \rho + Q_h + F + dF \quad (12)$$

Eq. (12) is further simplified by substituting Q_h and dF values from Eqs. (1) and (5), which yields

$$C_2 = \frac{1}{\sin \rho - \cos \rho \tan \phi} (C_1 - k_h dW - \tan \phi dV) \quad (13)$$

Summing up forces in the vertical direction, the following equation is then obtained as

$$V + dW = V + dV + S_1 + S_2 \sin \rho + C_2 \cos \rho + Q_v \quad (14)$$

Rearranging terms with substitution of Q_v , S_1 , S_2 , and C_2 , from Eqs. (2), (3), (4), and (13), respectively, Eq. (14) is reduced to

$$(1 - k_v + \cot(\rho - \phi) k_h) dW = (1 - \tan \phi \cot(\rho - \phi)) dV + (\tan \delta + \cot(\rho - \phi)) C_1 \quad (15)$$

To simplify the formulation, let a new coordinate system in terms y instead of z be defined as shown in Fig. 1. Namely

$$y = H - z \quad (16)$$

Substituting dW , dV , C_1 , and z values obtained from Eqs. (7), (9), (11), and (16), respectively, into Eq. (15), the following differential equation is thus obtained as

$$\frac{d\sigma_V}{dy} = \left[\frac{(\tan \delta + \cot(\rho - \phi)) \tan \rho}{1 - \cot(\rho - \phi) \tan \phi} K - 1 \right] \frac{\sigma_V}{y} - \left[\frac{1 - k_v + \cot(\rho - \phi) k_h}{1 - \cot(\rho - \phi) \tan \phi} \right] \gamma \quad (17)$$

A summary of the unknowns and equations used through the theoretical derivation of the suggested mathematical formulation is given in Table 1.

3. Solutions of differential equation

3.1 Horizontal pressure

Eq. (17) is a first order differential equation which can be written as

$$\frac{d\sigma_V}{dy} = (aK - 1) \frac{\sigma_V}{y} - b\gamma \quad (18)$$

in which the constants a and b are defined as

$$a = \frac{(\tan \delta + \cot(\rho - \phi)) \tan \rho}{1 - \cot(\rho - \phi) \tan \phi} \quad (19)$$

$$b = \frac{1 - k_v + \cot(\rho - \phi) k_h}{1 - \cot(\rho - \phi) \tan \phi} \quad (20)$$

The general solution of Eq. (18) is mathematically found to be

$$\sigma_V = Ny^{aK-1} + \frac{b\gamma}{aK-2} y \quad (21)$$

in which N is an integration constant. This constant is determined by using the following boundary condition.

$$\sigma_V(y = H) = 0 \quad (22)$$

Therefore the integration constant N is computed as

$$N = \frac{-b\gamma H^{2-aK}}{aK-2} \quad (23)$$

Substituting the constant N into the solution given by Eq. (21) and using Eq. (6), the horizontal lateral earth pressure σ_H acting on a retaining wall at any particular height y is defined as

$$\sigma_H = \frac{b\gamma K}{aK-2} \left[y - H^{2-aK} y^{aK-1} \right] \quad (24)$$

3.2 Resultant lateral earth force

The horizontal component of lateral earth force P_H , and the vertical shear force component P_V , acting on a retaining wall are obtained by integration as given by Eqs. (25) and (26). Namely

$$P_H = \int_0^H \sigma_H dy = \int_0^H \frac{b\gamma K}{aK-2} \left[y - H^{2-aK} y^{aK-1} \right] dy = \frac{1}{2} \gamma H^2 \frac{b}{a} \quad (25)$$

$$P_V = \int_0^H \sigma_H \tan \delta dy = \int_0^H \frac{b\gamma K}{aK-2} \left[y - H^{2-aK} y^{aK-1} \right] \tan \delta dy = \frac{1}{2} \gamma H^2 \frac{b}{a} \tan \delta \quad (26)$$

Since wall back is vertical, the resultant lateral earth force P is calculated from vector addition of the horizontal component P_H normal to the wall, and vertical shear force component P_V acting tangentially to the wall. Thus, P which makes an angle δ with the normal to wall back is obtained as

$$P = \sqrt{P_H^2 + P_V^2} = \frac{1}{2} \gamma H^2 \frac{b}{a \cos \delta} \quad (27)$$

3.3 Resultant lateral earth force position

The line of action y_r of the resultant lateral earth force P is obtained by dividing the lateral earth pressure moment M about wall base by the horizontal component of lateral force P_H as given by Eq. (28).

$$y_r = \frac{M}{P_H} \quad (28)$$

The lateral earth pressure moment M with respect to retaining wall base is obtained as

$$M = \int_0^H \sigma_H y dy = \int_0^H \frac{b \gamma K}{aK - 2} [y - H^{2-aK} y^{aK-1}] y dy = \frac{bK \gamma H^3}{3(aK + 1)} \quad (29)$$

Substituting P_H and M values obtained from Eqs. (25) and (29), respectively, into Eq. (28), the resultant lateral earth force line of action y_r is determined as

$$y_r = \frac{2aK}{3(aK + 1)} H = \left[\frac{1}{3} + \frac{aK - 1}{3(aK + 1)} \right] H \quad (30)$$

4. Illustrative example

The computations of lateral earth pressure distribution are illustrated by considering the data given in Fig. 1 with seismic conditions as $k_v = 0$ and $k_h = 0.2$. The two constants a and b are computed by Eqs. (19) and (20), respectively, as

$$a = \frac{(\tan 20 + \cot(77 - 30)) \tan 77}{1 - \cot(77 - 30) \tan 30} = 12.16 \quad (31)$$

$$b = \frac{1 - 0 + \cot(77 - 30) 0.2}{1 - \cot(77 - 30) \tan 30} = 2.57 \quad (32)$$

Using Eq. (24), lateral earth pressure distribution is plotted versus depth as shown in Fig. 2. For example, the lateral earth pressure value at a depth $z = 5$ m ($y = 4$ m) is calculated as

$$\sigma_H = \frac{2.57 \times 16 \times 0.3}{12.16 \times 0.3 - 2} [4 - 9^{2-12.16 \times 0.3} 4^{12.16 \times 0.3 - 1}] = 22.07 \text{ kN/m}^2 \quad (33)$$

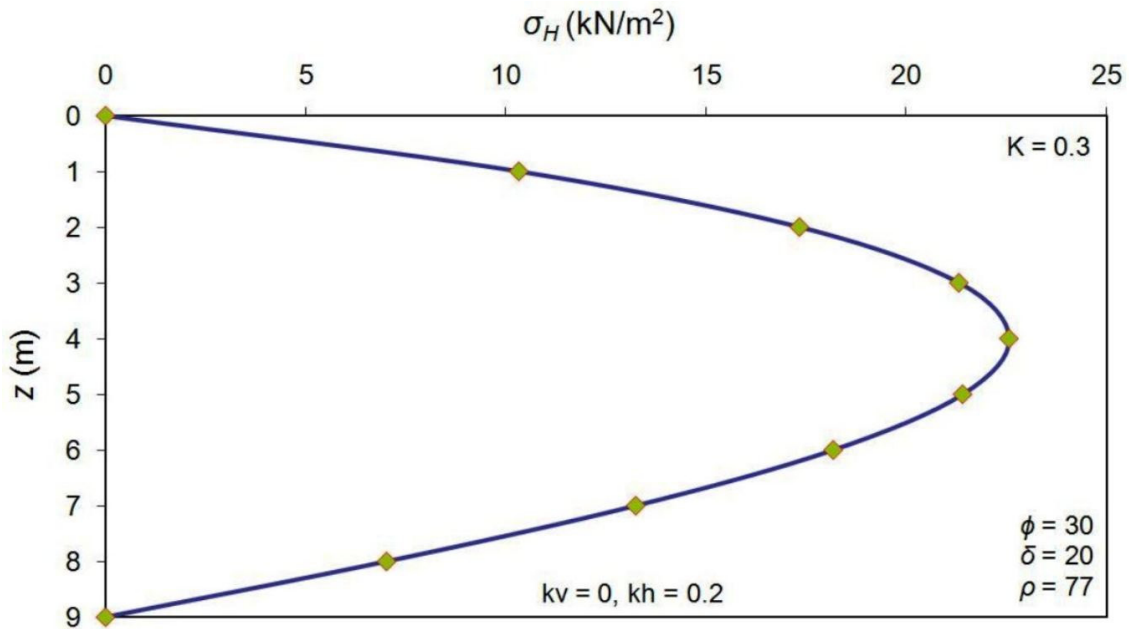


Fig. 2 Lateral earth pressure distribution with depth for the illustrative example

If Eqs. (27) and (30) are used directly to calculate the resultant lateral earth force and its line of action, respectively, the computations will be

$$P = \frac{1}{2}(16)(9)^2 \frac{2.57}{12.16 \cos 20} = 145.74 \text{ kN/m} \tag{34}$$

$$y_r = \frac{2 \times 12.16 \times 0.3}{3(12.16 \times 0.3 + 1)} 9 = 4.70 \text{ m} \tag{35}$$

5. Parametric study

As presented in Fig. 1, consider a retaining wall with $H = 9$ m, failure wedge width $B = 2$ m, failure wedge inclination $\rho = 77$ ($\cot^{-1} 2/9$), backfill unit weight $\gamma = 16 \text{ kN/m}^3$, friction angle $\phi = 30$, wall-to-soil friction angle $\delta = 20$, and lateral earth pressure coefficient $K = 0.3$. The effect of variation of several input parameters on lateral earth pressure distribution, and the position of the resultant lateral earth force, is investigated as illustrated below.

5.1 Horizontal and vertical acceleration coefficients

Influence of horizontal and vertical acceleration coefficients on lateral earth pressure of the wall is investigated using a classical method and the present formulation. Two sets of parameters are considered as follows: ($k_h = 0, 0.1, 0.2; k_v = 0$), and ($k_h = 0; k_v = 0.1, 0, -0.1$). Results are presented

in a graphical form for normalized lateral earth pressure (σ_H/H) with wall normalized depth (z/H) as shown in Figs. 3 and 4. The present research shows a nonlinear pattern of lateral earth pressure distribution as suggested by Eq. (24) while the classical theory shows a linear earth pressure distribution. It is seen that lateral earth pressure increases as k_h increases, decreases as k_v increases in the upwards direction, and increases as k_v increases in the downwards direction. Thus, the downwards direction of k_v is more critical and should be selected carefully with a negative sign when substituted into Eq. (20).

5.2 Lateral earth pressure coefficient

Influence of lateral earth pressure coefficient K on lateral earth pressure distribution and resultant lateral earth force line of action is investigated. Results of lateral earth pressure distribution with depth, for lateral earth pressure coefficients of 0.3, 0.4, and 0.5 are presented in Fig. 5. Generally, lateral pressure and nonlinearity degree increase with increase of lateral earth pressure coefficient K . In addition, as K increases lateral pressure in the upper zone of wall increases while slightly decreases close to wall base. Consequently, the resultant lateral earth force line of action y_r is shifted up from the wall. This is in agreement with Eq. (30) in which one can notice that the resultant lateral earth force line of action is always greater than one-third of wall height typically obtained from the classical theory. This in turn leads to a larger overturning moment against the retaining wall which influences wall stability and economy.

5.3 Soil friction angle

Based on the presently developed method, the variation of normalized lateral earth force ($P/0.5\gamma H^2$) with soil friction angle ϕ is presented in Fig. 6 for horizontal seismic coefficient $k_h = 0, 0.1, \text{ and } 0.2$, and in Fig. 7 for vertical seismic coefficient $k_v = 0, 0.1, \text{ and } 0.2$. It is noticed that lateral earth force shows a nonlinear decrease with increase in soil internal friction angle ϕ for all k_h and k_v values. It is seen that lateral earth force increases with the increase of horizontal seismic coefficient k_h while it decreases with the increase of vertical seismic coefficient k_v for all ϕ values.

5.4 Wall friction angle

Fig. 8 displays the variation of lateral earth force with soil friction angle ϕ for various wall-to-soil friction angles ($\delta = 10, 15, 20$). As illustrated, the resultant lateral earth force decreases as wall-to-soil friction angle δ increases for all ϕ values. The variation is significant for lower values of ϕ and becomes marginal as ϕ increases.

5.5 Failure plane angle

Influence of failure wedge inclination angle ρ (B/H ratio) is investigated in this research. Fig. 9 displays the normalized lateral earth pressure variation versus normalized depth for different B/H ratios. As seen, when the B/H ratio increases from 0.1 to 0.5 (ρ decreases), lateral earth pressure nonlinearity and magnitude increase as well. Figs. 10 and 11 show the normalized lateral earth force variation versus B/H ratio for various seismic accelerations. It is shown that the maximum lateral earth force occurs at a B/H ratio of about 0.7 indicating the critical slope of failure wedge angle ρ is in the order of 55 degrees.

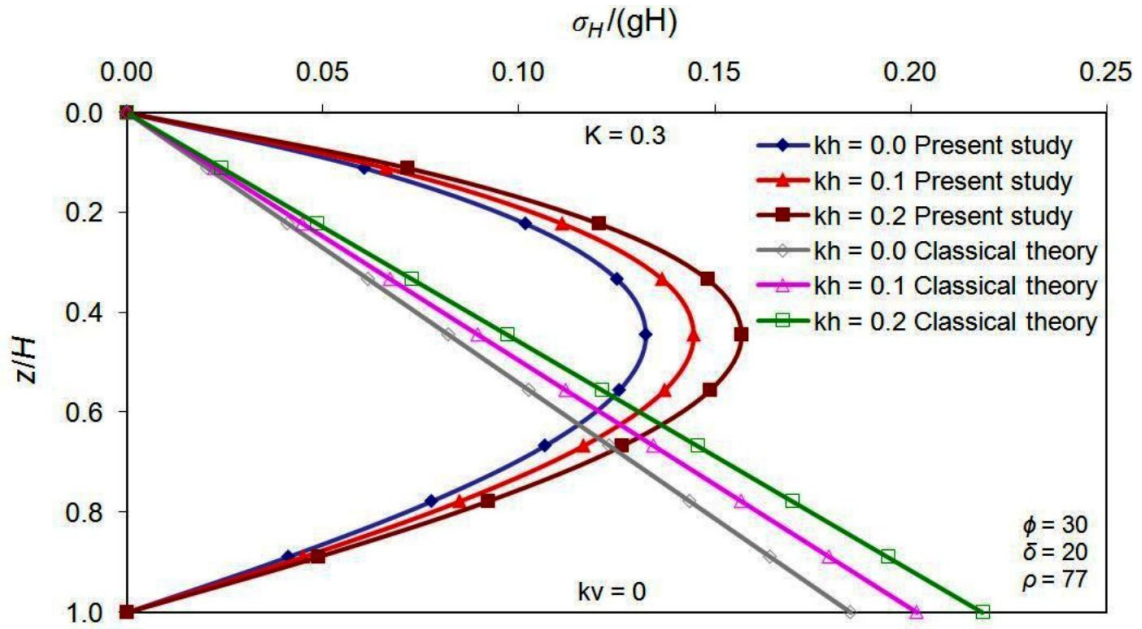


Fig. 3 Lateral pressure variation with depth for various horizontal seismic accelerations

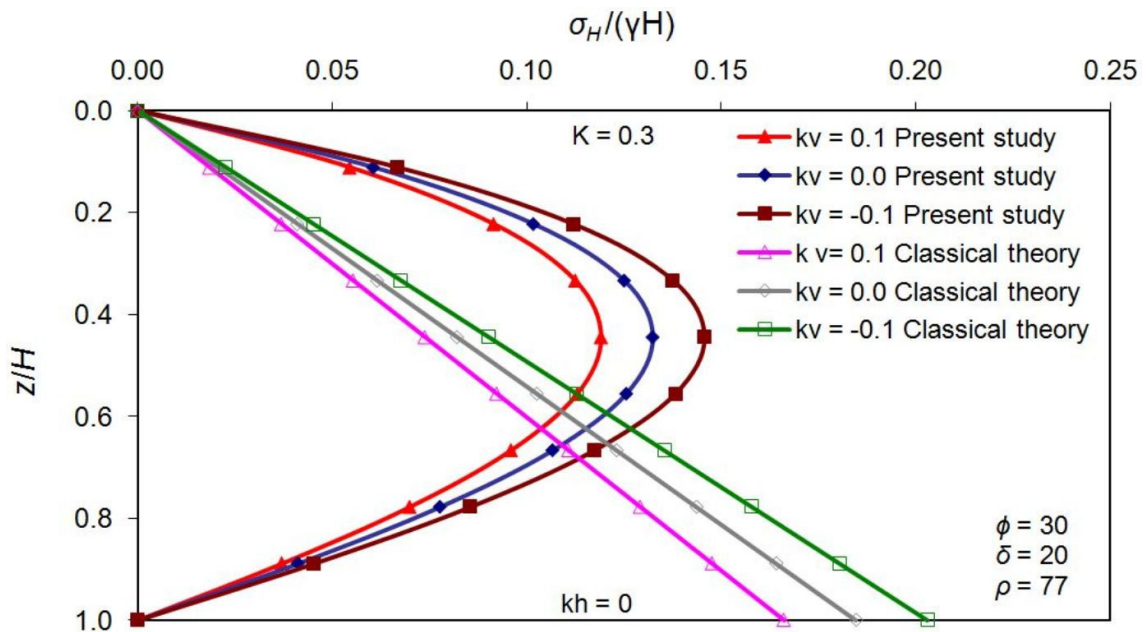


Fig. 4 Lateral pressure variation with depth for various vertical seismic accelerations

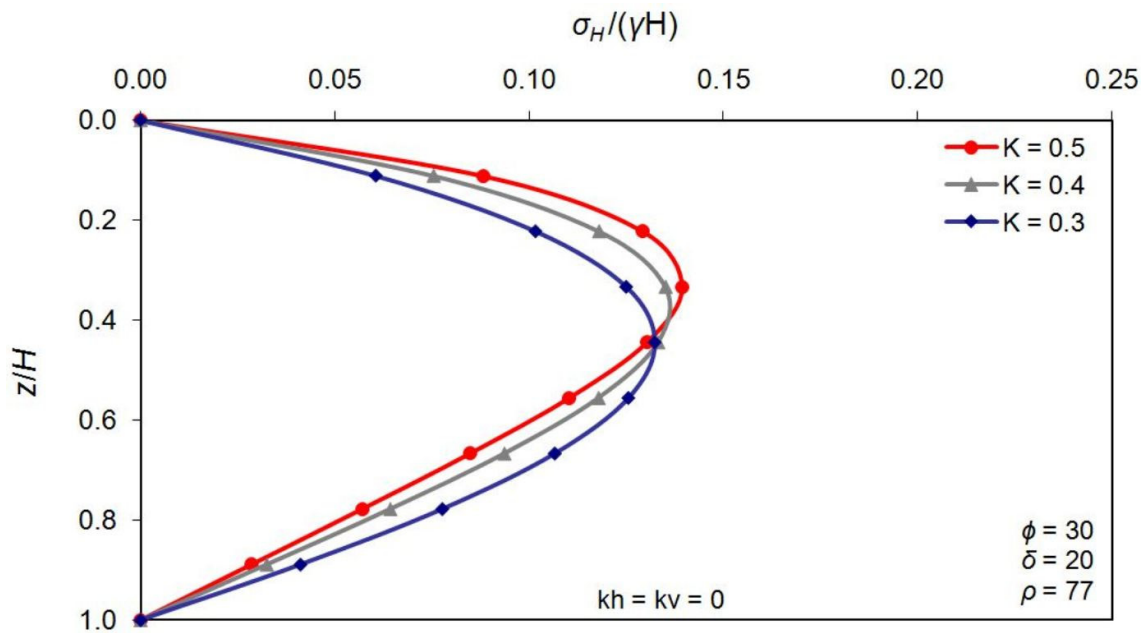


Fig. 5 Lateral pressure variation with depth for various lateral earth pressure coefficients

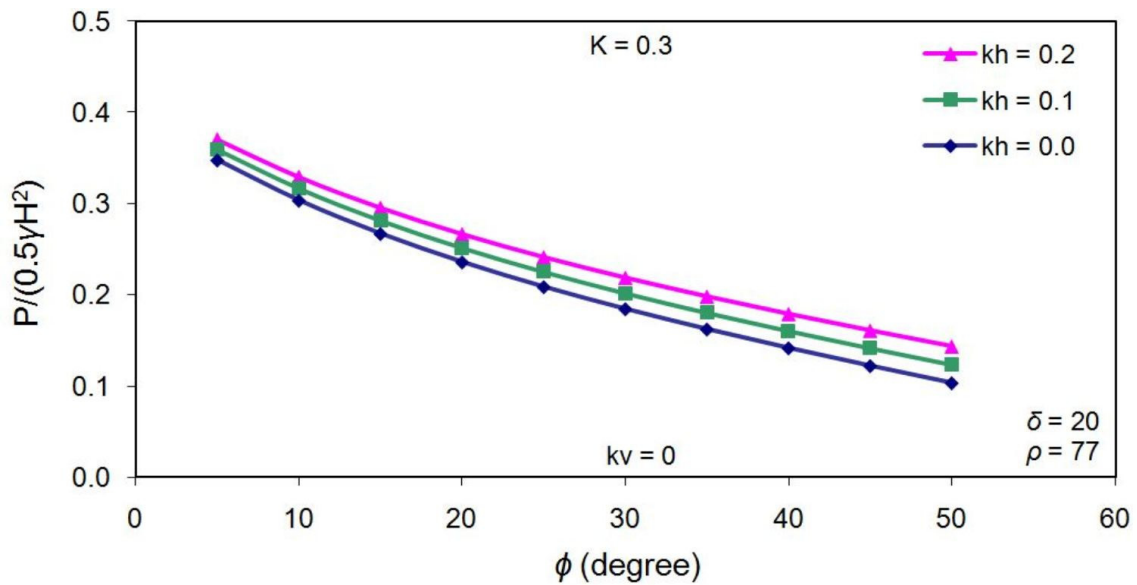


Fig. 6 Resultant force variation with soil friction angle for various horizontal seismic accelerations

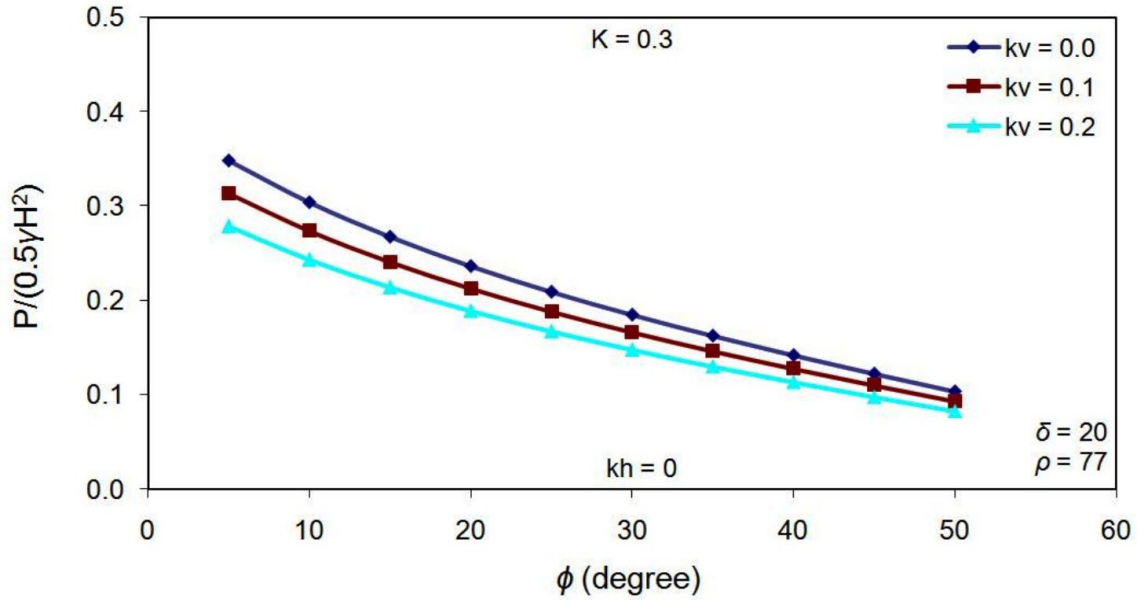


Fig. 7 Resultant force variation with soil friction angle for various vertical seismic accelerations

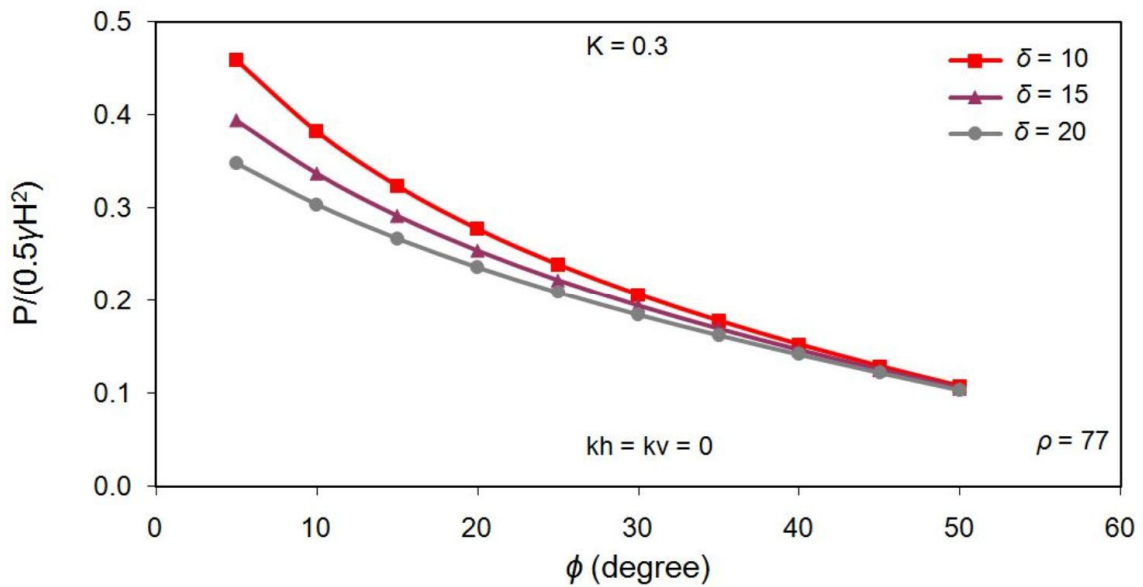


Fig. 8 Resultant force variation with soil friction angle for various wall-to-soil friction angles

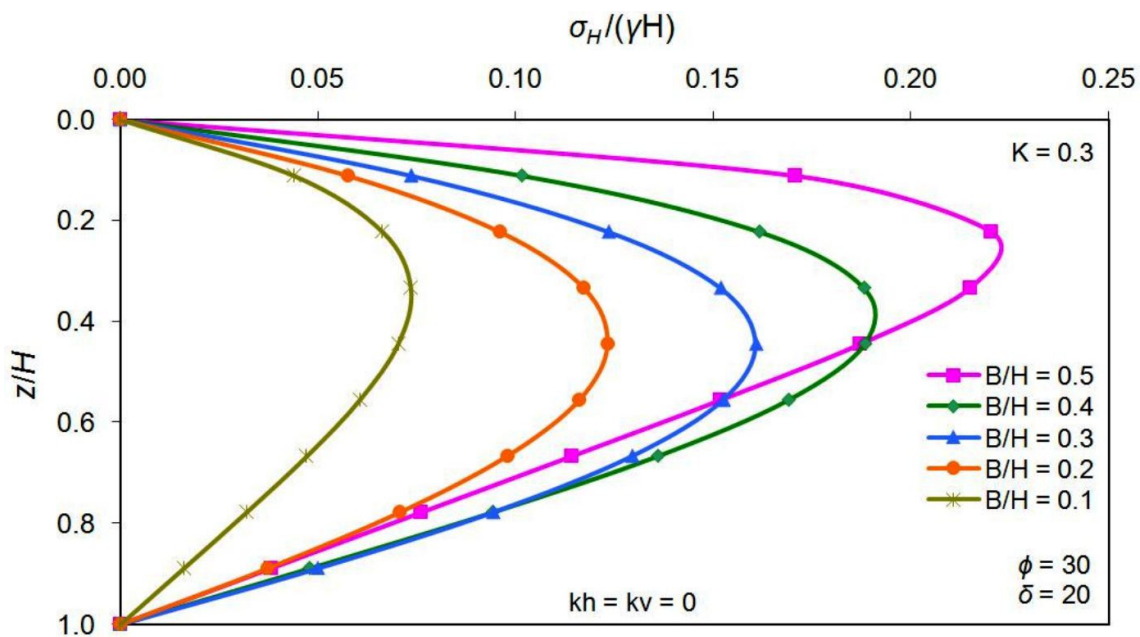


Fig. 9 Lateral pressure variation with depth for various B/H ratios

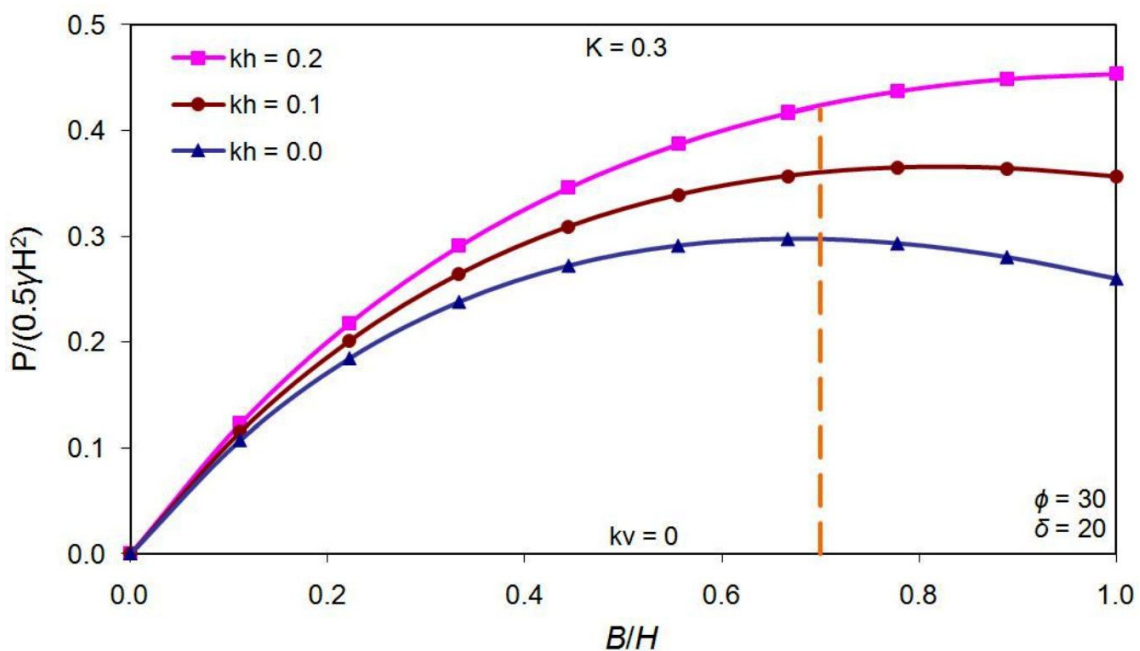


Fig. 10 Resultant force variation with B/H ratio for various horizontal seismic accelerations

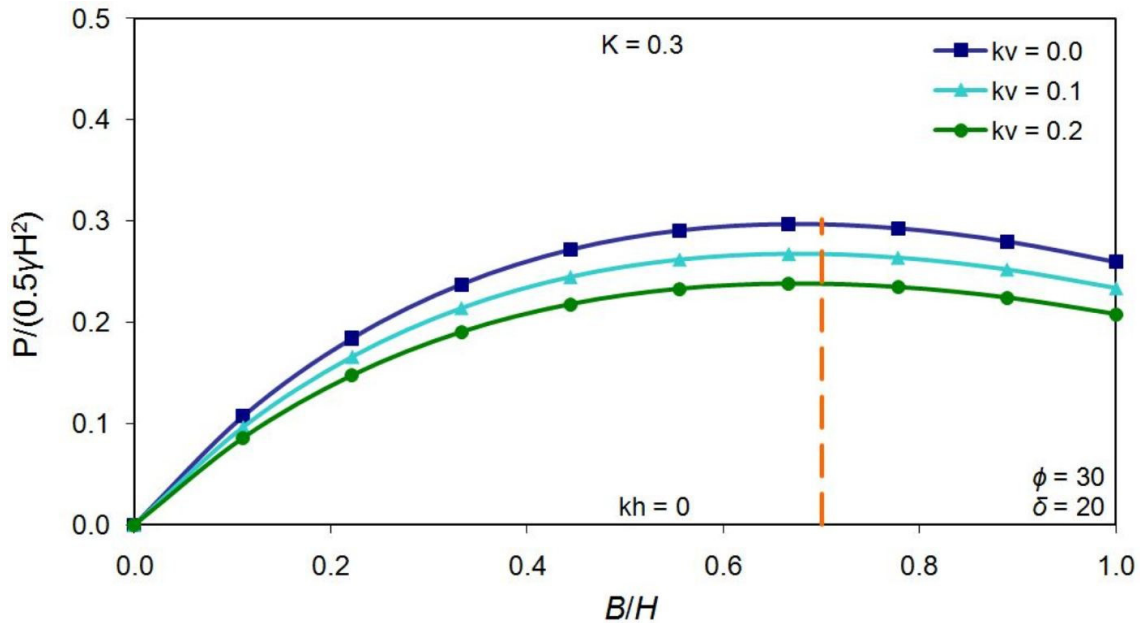


Fig. 11 Resultant force variation with B/H ratio for various vertical seismic accelerations

6. Comparison of results

A comparison between study findings with the classical M-O method, and Choudhury and Nimbalkar (2006), Ghosh (2010), and Giri (2011) studies is presented. The comparison is made for the variation of normalized lateral earth force behind a retaining wall for soil friction angle $\phi = 30$, wall-to-soil friction angle $\delta = 20$, and horizontal seismic coefficient $k_h = 0.1$ and 0.2 , versus different values of vertical seismic coefficient k_v .

As illustrated in Figs. 12 and 13, the normalized lateral earth force decreases by about 8.7% and 14.7% with the increase of vertical ground acceleration for $k_h = 0.1$ and 0.2 , respectively. And it increases by an average of 16.5% with the increase of horizontal ground acceleration from $k_h = 0.1$ to 0.2 . The results of the present study are in quite good agreement with the cited literature as the deviation of normalized lateral earth force is about 1.7% and 4.2% for horizontal ground acceleration $k_h = 0.1$ and 0.2 , respectively. Such deviation is attributed to the variant assumptions and boundary conditions made in the studies which are mainly related to wall rigidity, application and position of the seismic loads, and the direction of wall deformation and rotation.

The current study agrees with the cited literature (Choudhury and Nimbalkar 2006, Ghosh 2010, Giri 2011) in revealing that the seismic lateral earth pressure distribution behind a retaining wall is nonlinear as compared to the classical M-O method. As suggested by the present study, the nonlinear variation of seismic lateral earth pressure along wall depth is also reported by Fukuoka and Imamura (1984) with observed data for prototype retaining wall under earthquake condition, and with the experimental observations for model retaining wall under seismic conditions measured by Steedman and Zeng (1990).

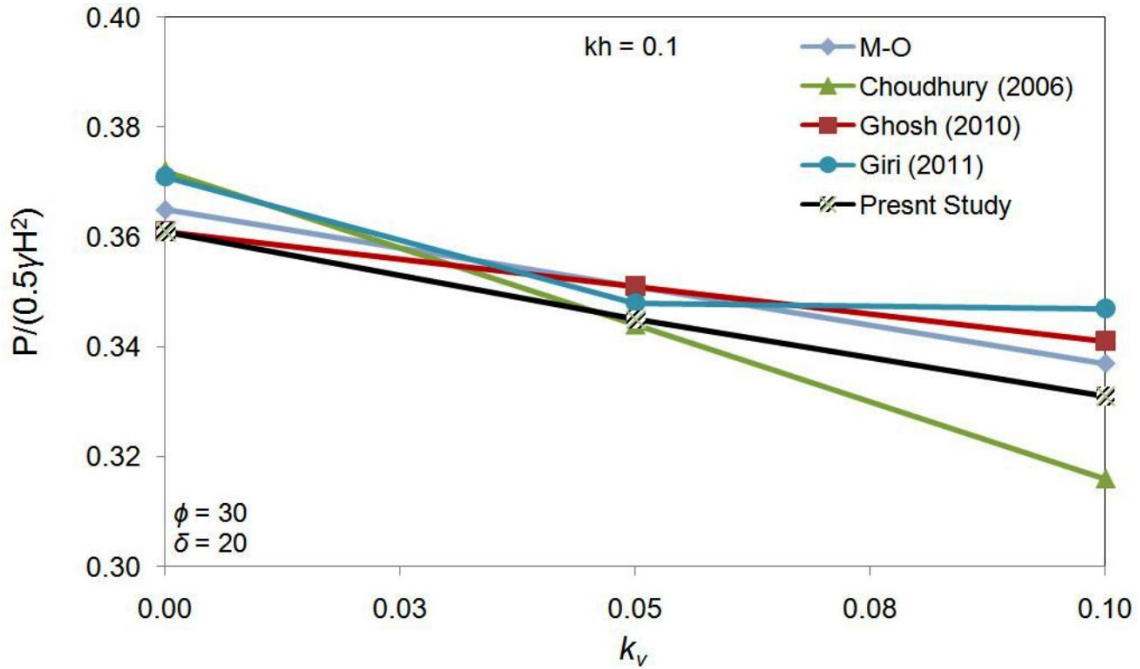


Fig. 12 Comparison of normalized lateral earth force by present study with literature ($k_h = 0.1$)

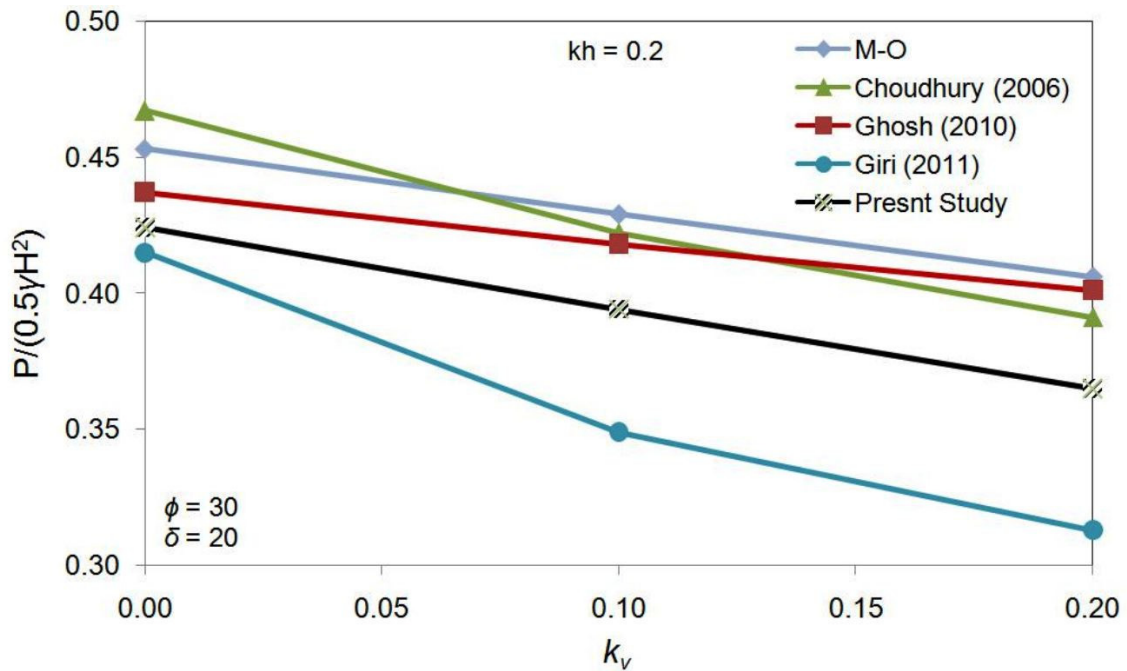


Fig. 13 Comparison of normalized lateral earth force by present study with literature ($k_h = 0.2$)

7. Conclusions

Based on limit equilibrium analysis, an alternative method is proposed to compute the lateral earth pressure distribution, and the resultant lateral earth force and its position. The theoretical expression considers the effects of gravitational and seismic loads for a vertical retaining wall supporting a granular soil. A parametric study is carried out to investigate the influence of several parameters on the magnitude and distribution of lateral earth pressure. A numerical example is presented to demonstrate the calculations of lateral earth pressure distribution with the proposed analytical formulation.

Lateral earth pressure distribution against a retaining wall is nonlinear along wall height for both gravitational and seismic conditions as compared to the linear distribution usually assumed with classical theory. For a particular retaining wall configuration, lateral earth pressure is influenced by the seismic acceleration level, and soil and wall properties. Generally, lateral earth pressure increases with the increase of horizontal seismic coefficient while it decreases with the increase of vertical seismic coefficient. The resultant lateral earth force line of action is located at an elevation higher than one-third of wall height being measured from its base. The height increases with the increase of lateral earth pressure coefficient. This in turn increases the overturning moment against the retaining wall which has a direct impact on wall stability and economy. The lateral earth pressure decreases with the increase of soil friction angle and wall roughness. The resultant lateral earth force increases with the decrease of failure wedge inclination until it reaches a maximum and then decreases.

8. Recommendations

Further investigation is required to account for layered soils, sloping backfill, inclined back wall, and surcharge load by modifying the theoretical derivation and boundary conditions appropriately.

Depending on the retaining wall movement and rigidity, the value of lateral earth pressure coefficient should be between active and at-rest conditions, and requires further investigation.

Additional finite element analysis and experimental testing program are needed to further verify and calibrate the suggested method.

Acknowledgments

The first author is grateful to The University of Jordan during which part of this study was conducted and for granting his leave. The additional research support complemented by Australian College of Kuwait is equally acknowledged.

References

- Ahmadabadi, M. and Ghanbari, A. (2009), "New procedure for active earth pressure calculation in retaining walls with reinforced cohesive-frictional backfill", *Geotext. Geomembr.*, **27**(6), 456-463.
- Bang, S. (1985), "Active earth pressure behind retaining walls", *J. Geotech. Eng.*, **111**(3), 407-412.
- Basha, B.M. and Babu, G.L.S. (2010), "Seismic rotational displacements of gravity walls by pseudo dynamic method with curved rupture surface", *Int. J. Geomech.*, **10**(3), 93-105.
- Bowles, J.E. (1996), *Foundation Analysis and Design*, McGraw Hill, New York, NY, USA.
- Caquot, A. and Kerisel, F. (1948), *Tables for the Calculations of Passive Pressure, Active Pressure and Bearing Capacity of Foundations*, Gauthier-Villars, Paris, France.
- Chen, W.F. and Liu, X.L. (1990), *Limit Analysis in Soil Mechanics: Developments in Geotechnical Engineering*, Elsevier, Amsterdam, Netherlands.
- Choudhury, D. and Nimbalkar, S.S. (2006), "Pseudo-dynamic approach of seismic active earth pressure behind a retaining wall", *Geotech. Geol. Eng.*, **24**(5), 1103-1113.
- Choudhury, D. and Singh, S. (2005), "New approach for estimation of static and seismic active earth pressure", *Geotech. Geol. Eng.*, **24**(1), 117-127.
- Coulomb, C.A. (1776), "Essai sur une application des regles de maximis et minimize a quelques problemes de stratique relatifs a l' architecture", *Memoires de mathematique et de physique, Presentes a l' academie royale des science (Mem. Acad. Roy. Div. Sav.)*, **7**, 343-387.
- Das, B.M. and Puri, V.K. (1996), "Static and dynamic active earth pressure", *Geotech. Geol. Eng.*, **14**(4), 353-366.
- Dewaikar, D.M. and Halkude, S.A. (2002), "Seismic passive/active thrust on retaining wall - point of application", *Soil. Found.*, **42**(1), 9-15.
- Fukuoka, M. and Imamura, Y. (1984), "Researches on retaining walls during earthquakes", *Proceedings of the 8th World Conference on Earthquake Engineering*, San Francisco, CA, USA, July, Volume 3, pp. 501-508.
- Ghanbari, A. and Taheri, M. (2012), "An analytical method for calculating active earth pressure in reinforced retaining walls subject to a line surcharge", *Geotext. Geomembr.*, **34**(1), 1-10.
- Ghosh, S. (2010), "Pseudo-dynamic active force and pressure behind battered retaining wall supporting inclined backfill", *Soil Dyn. Earthq. Eng.*, **30**(11), 1226-1232.
- Ghosh, S. and Sharma, R.P. (2010), "Pseudo-dynamic active response of non-vertical retaining wall supporting $c-\phi$ backfill", *Geotech. Geol. Eng.*, **28**(5), 633-641.
- Giri, D. (2011), "Pseudo-dynamic approach of seismic earth pressure behind cantilever retaining wall with inclined backfill surface", *Geomech. Eng., Int. J.*, **3**(4), 255-266.
- Ismeik, M. (2012a), "Practical evaluation of induced stress for calculation of consolidation settlement of soil", *Soil Mech. Found. Eng.*, **49**(3), 93-98.
- Ismeik, M. (2012b), "Stress increment solution charts for soil consolidation analysis", *Global J. Res. Eng.*, **12**(4), 13-17.
- Ismeik, M. and Al-Rawi, O. (2014), "Modeling soil specific surface area with artificial neural networks", *Geotech. Test. J.*, **37**(4), 678-688.
- Ismeik, M., Ashteyat, A.M. and Ramadan, K.Z. (2013), "Stabilisation of fine-grained soils with saline water", *Eur. J. Environ. Civil Eng.*, **17**(1), 32-45.
- Lee, I.K. and Herrington, J.R. (1972), "A theoretical study of the pressure acting on a rigid wall by sloping earth or rock fill", *Geotechnique*, **22**(1), 1-27.
- Mononobe, N. and Matsuo, H. (1929), "On the determination of earth pressure during earthquakes", *Proceedings of the World Engineering Congress*, Tokyo, Japan, October, Volume 9, pp. 177-185.
- Nouri, H., Fakher, A. and Jones, C.J.F.P. (2006), "Development of horizontal slice method for seismic stability analysis of reinforced slopes and walls", *Geotext. Geomembr.*, **24**(3), 175-187.
- Nouri, H., Fakher, A. and Jones, C.J.F.P. (2008), "Evaluating the effects of the magnitude and amplication of pseudo-static acceleration on reinforced soil slopes and walls using the limit equilibrium horizontal slices method", *Geotext. Geomembr.*, **26**(3), 263-278.

- Okabe, S. (1926), "General theory of earth pressure and seismic stability of retaining walls and dams", *J. Japan. Soc. Civil Eng.*, **10**(6), 1277-1288.
- Perkins, S., Ismeik, M. and Fogelsong, M. (1998), "Mechanical response of a geosynthetic-reinforced pavement system to cyclic loading", *Proceedings of the 5th International Conference on the Bearing Capacity of Roads and Airfields*, Trondheim, Norway, July, Volume 3, pp. 1503-1512.
- Rankine, W.J.M. (1857), "On the mathematical theory of the stability of earthwork and masonry", *Proceedings of the Royal Society of London*, London, UK, June, Volume 8, pp. 60-61.
- Shahgholi, M., Fagher, A. and Jones, C.J.F.P. (2001), "Horizontal slice method of analysis", *Geotechnique*, **51**(10), 881-885.
- Shekarian, S., Ghanbari, A. and Farhadi, A. (2008), "New seismic parameters in the analysis of retaining walls with reinforced backfill", *Geotext. Geomembr.*, **26**(4), 350-356.
- Sherif, M.A., Ishibashi, I. and Lee, C.D. (1982), "Earth pressure against rigid retaining walls", *J. Geotech. Eng.*, **108**(GT5), 679-695.
- Shukla, S.K. and Zahid, M. (2011), "Analytical expression for dynamic active earth pressure from $c-\phi$ soil backfill with surcharge", *Int. J. Geotech. Eng.*, **5**(2), 143-150.
- Shukla, S.K., Gupta, S.K. and Sivakugan, N. (2009), "Active earth pressure on retaining wall for $c-\phi$ soil backfill under seismic loading condition", *J. Geotech. Geoenviron. Eng.*, **135**(5), 690-696.
- Sokolovski, V.V. (1965), *Statics of Granular Media*, Pergamon, London, UK.
- Steedman, R.S. and Zeng, X. (1990), "The influence of phase on the dilution of pseudo-static earth pressure on a retaining wall", *Geotechnique*, **40**(1), 103-112.
- Terzaghi, K. (1943), *Theoretical Soil Mechanics*, Wiley, New York, NY, USA.
- Wang, Y.Z. (2000), "Distribution of earth pressure on a retaining wall", *Geotechnique*, **50**(1), 83-88.
- Wang, Y.Z., Tang, Z.P. and Zheng, B. (2004), "Distribution of active earth pressure of retaining wall with wall movement of rotation about top", *Appl. Math. Mech.*, **25**(7), 761-767.

Nomenclature

a	integration constant (dimensionless)
b	integration constant (dimensionless)
A	soil area (m ²)
B	failure wedge top width (m)
C_1	wall-to-soil normal compressive force (kN)
C_2	soil normal compressive force (kN)
F	horizontal shearing force (kN)
H	retaining wall height (m)
K	lateral earth pressure coefficient (dimensionless)
k_h	horizontal seismic acceleration coefficient (dimensionless)
k_v	vertical seismic acceleration coefficient (dimensionless)
M	earth pressure moment to wall base (kN.m)
N	integration constant (dimensionless)
P	resultant lateral earth force (kN)
P_H	horizontal component of lateral earth force (kN)
P_V	vertical component of lateral earth force (kN)
Q_h	horizontal seismic inertia force (kN)
Q_v	vertical seismic inertia force (kN)
S_1	tangential wall-to-soil shearing force (kN)
S_2	tangential soil shearing force (kN)
V	internal vertical soil force (kN)
W	soil weight (kN)
y	height above wall bottom surface (m)
y_r	resultant lateral earth force line of action (m)
z	depth below wall top surface (m)
ϕ	soil friction angle (degrees)
ρ	failure wedge inclination to horizontal (degrees)
γ	backfill soil unit weight (kN/m ³)
δ	wall-to-soil friction angle (degrees)
σ_H	horizontal pressure (kN/m ²)
σ_V	vertical pressure (kN/m ²)